Lassa virus NP DEDDh 3'-5' exoribonuclease activity is required for optimal viral RNA replication and mutation control.

Cheng Huang[1]*, Emily Mantlo[1,2,] Slobodan Paessler[1]

[1]Department of Pathology, Galveston National Laboratory and Institute for Human Infections and Immunity, University of Texas Medical Branch, Galveston, TX, USA

[2] Current address: Department of Microbiology & Immunology, Upstate Medical University, Syracuse, NY, USA.

*Corresponding Author:

Email: chhuang@utmb.edu

Abstract

Lassa virus (LASV), a mammarenavirus from *Arenaviridae*, is the causative agent of Lassa fever (LF) endemic in West Africa. Currently, there are no vaccines or antivirals approved for LF. The RNA-dependent RNA polymerases (RdRp) of RNA viruses are error-prone. As a negative-sense RNA virus, how LASV copes with errors in RNA synthesis and ensures optimal RNA replication are not well elucidated. LASV nucleoprotein (NP) contains a DEDDH 3'-to-5' exoribonuclease motif (ExoN), which is known to be essential for LASV evasion of the interferon response via its ability to degrade virus-derived double-stranded RNA. Herein, we present evidence that LASV NP ExoN has an additional function important for viral RNA replication. We rescued an ExoN-deficient LASV mutant (ExoN- rLASV) by using a reverse genetics system. Our data indicated that abrogation of NP ExoN led to impaired LASV growth and RNA replication in interferon-deficient cells as compared with wild-type rLASV. By utilizing PacBio Single Molecule, Real-Time (SMRT) long-read sequencing technology, we found that rLASV lacking ExoN activity was prone to producing aberrant viral genomic RNA with structural variations. In addition, NP ExoN deficiency enhanced LASV sensitivity to mutagenic nucleoside analogues in virus titration assay. Next-generation deep sequencing analysis showed increased single nucleotide substitution in ExoN-LASV RNA following mutagenic 5-flurouracil treatment. In conclusion, our study revealed that LASV NP ExoN is required for efficient viral RNA replication and mutation control. Among negative-sense RNA viruses, LASV NP is the first example that a viral protein, other than the RdRp, contributes to reduce errors in RNA replication and

maintain genomic RNA integrity. These new findings promote our understanding of the basics of LASV infection and inform antiviral and vaccine development.

Authors Summary

Lassa fever (LF) is a severe and often fatal disease endemic in West Africa. There is no vaccines or antivirals approved for LF. The disease is caused by Lassa virus (LASV), a member of the arenavirus family. LASV nucleoprotein (NP) contains a DEDDh exoribonuclease (ExoN) motif, through which NP degrades virus-derived, immunostimulatory double-stranded RNA and inhibit host innate immune response. Thus, it is well known that NP ExoN is important for LASV pathogenicity. Intriguingly, the NP ExoN motif is highly conserved among arenaviruses, regardless of pathogenicity and viral ability to evade innate immune response, suggesting arenavirus NP ExoN may have additional function(s) in virus infection. In this study, we found that loss of ExoN activity affected LASV multiplication and RNA replication in interferon-deficient Vero cells. The ExoN-deficient rLASV exhibited reduced level of viral RNA, increased frequency of structural variation in virus genomic RNA, and higher mutation rate following mutagenic nucleoside analogue treatment. In conclusion, LASV NP ExoN plays an important role in viral RNA replication and fitness. Our new findings may inform antiviral and vaccine development and have broader implication on the function of NP ExoN of other arenaviruses.

Introduction

The *Arenaviridae* family consists of four genera: *Mammarenavirus*, *Reptarenavirus*, *Hartmanivirus*, and *Antennavirus (1, 2)*. *Mammarenaviruses* (referred to as

arenaviruses hereafter) contain several pathogens of major clinical importance. Lassa virus (LASV) causes Lassa fever (LF), which is endemic in West Africa (3-6). The New World arenaviruses Junín virus (JUNV) and Machupo virus (MACV) cause Argentine hemorrhagic fever (AHF) and Bolivian hemorrhagic fever (BHF), respectively, in South America (7-10). These arenaviruses normally infect their rodent hosts, often persistently without overt disease signs. Spillover to humans occurs through aerosol inhalation and causes severe zoonotic diseases, of which vaccines and antivirals are limited (3, 8, 11-13). Accordingly, LASV, JUNV and MACV are classified as Category A Priority Pathogens in the USA. The World Health Organization has listed LF in the Blueprint list of priority diseases for which there is an urgent need for accelerated research and development (14).

Arenaviruses are negative-sense RNA viruses with a single-stranded, bi-segmented RNA genome (15). The large (L) segment RNA and the small (S) segment RNA are around 7.3 kb and 3.4 kb in length (Fig 1A). The L RNA encodes the RNA-dependent RNA polymerase (RdRp) L protein and a small, zinc finger protein (Z), which drives the assembly and budding of virus particles. The S RNA encodes the viral glycoprotein (GP), which mediates virus entry into host cells, as well as the nucleoprotein (NP), which is the major structural component of the nucleocapsid. On each genomic RNA, there is a highly structured, GC-rich intergenic region (IGR) (Fig 1A), which is the termination signal for viral mRNA transcription and is also required for packaging of viral genomic RNA into progeny virus particles (16). After virus entry, NP mRNA and L mRNA are transcribed from the 3'-end of S genomic RNA (S gRNA) or L genomic RNA (L gRNA), respectively (Fig 1B). Later in infection, S anti-genomic RNA (S agRNA) and

L anti-genomic RNA (L agRNA) are synthesized from S gRNA and L gRNA, which are the templates for GPC mRNA and Z mRNA transcription as well as S gRNA and L gRNA synthesis (Fig 1B).

The RNA polymerase of RNA virus lacks proofreading activity. As negative sense RNA viruses, how arenaviruses control errors in RNA replication are not well elucidated. Both RdRp L protein and NP are required for viral RNA replication (17, 18), which occurs in virus-induced, discrete cytosolic structures (19). Arenavirus NP contains two structurally and functionally separated domains. The N-terminal half (aa 1-340 in LASV NP) binds to viral genomic RNA to form vRNP (20). In the C-terminal half of LASV NP, D389, E391, D466, D533 and H528 constitute a DEDDh 3'-5' exoribonuclease (ExoN)-like motif. Structural and biochemical studies have established that the LASV NP harbors exoribonuclease activity specific for double-stranded RNA (dsRNA). Mutation of any of these DEDDh residues abolishes the ExoN activity (21-23). NP ExoN-mediated dsRNA degradation is essential for LASV NP inhibition of the Sendai virus-induced interferon response (21, 23), which is consistent with LASV suppression of the innate immune response *in vitro* and *in vivo.* It is widely accepted that LASV NP ExoN is critical for LASV immune evasion and pathogenicity (24, 25).

Interestingly, the NP DEDDh motif and its 3'-5' ExoN activity are highly conserved in arenaviruses regardless of pathogenicity and virus ability to evade IFN response. For instance, the ExoN motif is also found in the NP of the non-pathogenic Tacaribe virus (TCRV), Pichinde virus (PICV) and Mopeia virus (MOPV) (22, 26-30). Notably, it has been shown that abrogation of ExoN activity impaired the ability of NP to support LASV minigenome replication (31, 32), suggesting a role of NP ExoN in arenavirus lifecycle

aside from immune evasion. Interestingly, the nsp14 protein of the positive-sense RNA coronavirus also possesses the same DEDDh ExoN motif, which is essential for the fidelity of coronavirus RNA replication (33-35). Thus, further studies are warranted to investigate whether LASV NP ExoN plays a role in viral RNA replication in addition to immune evasion.

In the present study, we rescued an ExoN-deficient mutant LASV (ExoN- rLASV) and found that loss of ExoN activity resulted in impaired virus growth and viral RNA replication in interferon-deficient cells. Our study also showed that abrogation of NP ExoN led to increased production of aberrant LASV RNA and higher sensitivity to mutagenic nucleoside analogues as compared with wild-type LASV. These data present evidence that LASV NP ExoN has an important function in viral RNA replication in addition to its role in immune evasion. Our new findings may enhance our understanding of the basic virology of this important human pathogen and open new directions for future studies.

Results

Abrogation of NP ExoN activity impaired LASV multiplication in interferon-deficient cells.

In biochemical studies, mutation of any of the LASV NP D389, E391, D466, D533 and H528 residues to alanine diminished the ExoN activity. Accordingly, we attempted to rescue recombinant LASV (rLASV, Josiah strain) harboring NP D389A and NP D389AG392A mutations to investigate the role of LASV ExoN in infection. To minimize the likelihood of reversion, two nucleotide substitutions were introduced to mutate the

NP D380 and NP G392 residues. Specifically, for the NP D380A mutant, nt $GA_{1266}C_{1267}$ in S RNA (in antigenomic sense) was mutated to $GC_{1266}T_{1267}$. For the NP D389AG392A mutant, $GA_{1266}C_{1267}$ (D389) and $GG_{1275}A_{1276}$ (G392) in S RNA were mutated to $GC_{1266}T_{1267}$ (D389A) and $GC_{1275}T_{1276}$ (G392A), respectively. We successfully rescued the rLASV NP D389A mutant (ExoN- rLASV hereafter) by using the reverse genetics systems established in our lab. Sequencing analysis confirmed that the mutation is stable after 3 passages in Vero cells (Fig 2A). We could not rescue the rLASV NP D389AG392A mutant despite repeated attempts, indicating rLASV with the NP D389AG392A mutation is not viable.

We assessed the one-step and multiple-step growth kinetics of ExoN- rLASV in interferon-deficient Vero cells. The multiplication of ExoN- rLASV was attenuated at both conditions as compared with wild-type (wt) rLASV (Fig 2B). At 48 hours post-infection (hpi), the titer of ExoN- rLASV was 835-fold lower than wt rLASV at MOI 1, and 51-fold lower at MOI 0.01. Consistently, ExoN- rLASV formed smaller plaques in Vero cells as compared with wt rLASV (Fig 2C). These results indicated that abrogation of ExoN activity impaired rLASV propagation in Vero cells.

NP ExoN deficiency impaired LASV RNA replication in interferon-deficient cells.

As Vero cells are IFN-deficient (36, 37), the attenuated growth of ExoN- rLASV in Vero cells suggests that NP ExoN plays an important role in LASV replication other than viral evasion of the IFN response. We reasoned that ExoN deficiency may affect LASV RNA replication like its coronavirus nsp14 counterpart and further examined LASV RNA replication in Vero cells at conditions representing one-step virus growth (MOI 1 for 24 hr) and multi-step growth (MOI 0.01 for 72 hr). As shown in Fig 3A, the titer of ExoN-

rLASV was 6671-fold lower than that of wt rLASV at MOI 1 and was 51.4-fold lower at MOI 0.01. We purified total RNA from infected cells and performed reverse transcription with random primers. Then, we conducted a qPCR assay to quantify the viral RNA level at the NP locus, which measures the total RNA level of S gRNA, S agRNA and NP mRNA (Fig 3B). Similarly, we also determined the RNA level of L gRNA, L agRNA and L mRNA with a qPCR assay using primers specific for the L locus (Fig 3C). At a MOI of 1, which represents one-step virus growth, the RNA level of ExoN- rLASV RNA was 1637-fold lower than that of wt rLASV at the NP locus ($P<0.01$, student t test), and 122-fold lower ($P<0.01$) at the L locus. At a MOI of 0.01, which represents multi-step virus growth, the RNA level of ExoN- rLASV was 45.5-fold lower than that of wt rLASV at the NP locus ($P<0.01$, student t test), and 25.2-fold lower at the L locus ($P=0.04$, student t test).

We also examined the impact of ExoN deficiency on the level of S and L genomic RNA by RT-qPCR assay. In this assay, reverse transcription was performed with primers targeting the 3'-end of S genomic RNA and L genomic RNA using the high-fidelity reverse transcriptase SuperScript IV (Invitrogen), followed by qPCR assays targeting the NP locus on S gRNA and the L locus on L gRNA. At the one-step growth condition (MOI of 1), the level of ExoN- rLASV S gRNA was 1181-fold lower ($P<0.01$, t test) than that of wt rLASV; meanwhile the level of L gRNA was 387-fold lower ($P<0.02$) (Fig 3D and 3E). At a MOI of 0.01, the level of ExoN- rLASV S gRNA was 62.3-fold lower ($P<0.01$, t test) than that of wt rLASV; meanwhile the level of L gRNA was16.7-fold lower ($P<0.02$) than that of wt rLASV. These results clearly demonstrated that

abrogation of ExoN affected LASV RNA level in IFN-deficient Vero cells, to an extent largely comparable with virus titer reduction.

Abrogation of ExoN led to increased aberrant viral RNA formation in rLASV infection.

Next, we performed RT-PCR to examine S gRNA and L gRNA in ExoN- rLASV infection. Vero cells were infected with wt rLASV and ExoN- rLASV at a MOI of 0.01 for 72 hours or at a MOI of 1 for 24 hours. Intracellular RNA samples were purified and reverse transcribed to cDNA using primers targeting the 3'-ends of S gRNA or L gRNA. Nearly full-length S gRNA (3391 nt) and L gRNA (7265 nt) was amplified with the high-fidelity Platinum SuperFi DNA Polymerase (Invitrogen). In agarose electrophoresis, we observed an aberrant S RNA product (indicated as S' in Fig 4A) migrating slightly faster than the standard S gRNA product (3391 nt) in ExoN- rLASV samples at both a MOI of 0.01 and 1. The aberrant S' product was detected specifically in ExoN- rLASV infection in repeated experiments. We also observed several aberrant L gRNA products (3.5 kb to 6 kb) in ExoN- rLASV samples at both a MOI of 0.01 and 1 (Fig 4B). These results demonstrated increased formation of aberrant S gRNA and L gRNA in ExoN- rLASV infection.

Abrogation of LASV NP ExoN activity affected the integrity of S gRNA.

To determine the sequence of the aberrant S' RNA in ExoN- rLASV infection, we performed agarose gel electrophoresis with ExoN- rLASV and wt rLASV S RNA PCR samples (MOI of 1) and purified the amplicons around the full size of S segment. Purified amplicons were cloned into a cloning vector (pSMART, Lucigen). Sanger sequencing of ten colonies identified two types of aberrant S RNAs formed in ExoN-

rLASV infection. Three out of ten colonies had a 37-nt deletion (corresponding to nt1824-1860 in S agRNA), shown as the region from site I to site I' in Fig 5A and 5B. The 37-nt deletion in the 67-nt-long IGR could disrupt the stem-loop structure of the IGR. In addition, five colonies contained a 231-nt deletion spanning the IGR and NP coding region (nt1616-1846 in S agRNA, from site II to II' in Fig 5C). The 231-nt deletion consists of 42 nt in the IGR and 189 nt at the 3' end of the NP gene (Fig 5C), which could disrupt IGR structure and cause an open reading frame shift from NP residue 507. In comparison, only two out of 10 colonies in the wt rLASV S samples had the 37-nt deletion in IGR, while the remaining colonies had the correct sequence. These data indicated that LASV lacking NP ExoN is more prone to forming structural deletion in S RNA, particularly around the IGR.

PacBio Single Molecule, Real-Time (SMRT) long-read sequencing to characterize aberrant S gRNA formed in ExoN- rLASV infection.

To systematically assess the spectrum of aberrant S gRNA formed in ExoN- rLASV infection, we utilized PacBio Single Molecule, Real-Time (SMRT) long-read sequencing technology (38) to characterize LASV SgRNA at the single-molecule level. In PacBio SMRT long-read sequencing, a DNA polymerase continues to read a single circularized cDNA template for multiple rounds and provides deep sequencing data for each molecule. It can determine the circular consensus sequence (CCS) of full-length cDNA up to 10kb long at the single-molecule level with up to 99.99% accuracy. PacBio SMRT long-read sequencing is ideal for analyzing RNA quasi-species, long amplicons, and structural variations. It has been successfully used in studies on defective-interfering

RNA in influenza virus infection and hepatitis C virus variants following drug treatment (39, 40).

We gel purified the nearly full-length S RNA PCR amplicon from wt- and ExoN- rLASV-samples (MOI of 1) and performed PacBio SMRT long-read sequencing (Sequel II). A total of 402,410 CCS reads and 381,134 CCS reads were obtained for wt rLASV and ExoN- rLASV samples, respectively (Fig 6A). The mean number of read passes for each cDNA was 28 times for wt rLASV (average length of 2319 nt) and 26 times for ExoN- rLASV (average length of 2610 nt) (Fig 6A). The mean read score of the assay was >0.999. CCS reads with a size of 3100-3391 bp were selected using Filter FASTQ and aligned with the LASV reference sequence using *minimap2* (41). Variants with higher than 3% frequency were called using *iVar* (42). In the ExoN- rLASV sample, we found that 88.9% and 4.9% of S RNA had the 231-nt and the 37-nt deletion, respectively (Fig 6B and 6C). In comparison, 7.1% and 18.2% of the S RNA in the wt rLASV sample had the 231-nt and the 37-nt deletion, respectively. The data also confirmed that greater than 99.93% of ExoN- rLASV harbored the intended NP D389A mutation. In addition, an A-to-G substitution at nt 393 (in antigenomic sense) was identified in S RNA of ExoN- rLASV with a frequency of 36.7%. A C-to-U substitution at nt 1518 in S RNA was found in wt rLASV sample with a frequency of 3.07%. Overall, a systematic analysis with PacBio SMRT sequencing clearly showed that LASV lacking ExoN had a higher frequency of structural variation in S gRNA.

ExoN- rLASV was more sensitive to nucleoside analogue treatment.

Coronavirus nsp14 DEDDh 3’-5’ ExoN proofreads newly synthesized viral RNA by removing mis-incorporated nucleotides. Abrogation of nsp14 ExoN activity renders

coronaviruses susceptible to lethal mutagenesis when treated with nucleoside analogues such as 5-fluorouracil (5-FU) (43). 5-FU treatment also increases the mutation rate of the prototype arenavirus lymphocytic choriomeningitis virus (LCMV) and affects viral fitness (44). To investigate if loss of ExoN activity could increase LASV sensitivity to mutagenic nucleoside analogues, we evaluated the sensitivity of wt rLASV and ExoN- rLASV to 5-FU in Vero cells (MOI of 0.1). 5-FU treatment alone did not affect cell viability at the concentrations administrated in this experiment (Fig. 7A, CellTiter-Glo Viability Assay, Promega). Abrogation of NP ExoN increased LASV sensitivity to 5-FU treatment starting from 100 µM (Fig 7B). At 400 µM, the virus titer of ExoN- rLASV deceased by 1053-fold as compared with mock treatment, which was 13.5-times greater than the 78-fold decrease for wt rLASV (Fig 7B).

EIDD-1931 (*N4*-hydroxycytidine or NHC) is a cytidine analogue that increases the mutation frequency of a broad range of RNA viruses (45). We also assessed the sensitivity of ExoN- rLASV and wt rLASV to EIDD-1931. EIDD-1931 treatment alone (5 µM-100 µM) did not substantially affect cell viability (Fig 7A, CellTiter-Glo Viability Assay, Promega). The titer of ExoN- rLASV was decreased by 47.6-fold following 100 µM EIDD-1931 treatment, greater than the 6-fold reduction of wt rLASV at the same condition (Fig 7C). Collectively, these results indicated that abrogation of NP ExoN activity rendered LASV more sensitive to mutagenic nucleoside analogues.

Increased rate of single nucleotide variation in ExoN- rLASV RNA following 5'-FU treatment.

We further assessed the impact of the loss of ExoN on the mutation rate of LASV RNA following 5-FU treatment. We infected Vero cells with rLASV (MOI 0.1) and treated

cells with a low level of 5-FU (100 μM). Extracted viral RNAs were reverse transcribed with primers specific to S genomic and L genomic RNA. We performed high-fidelity PCR to generate two overlapping amplicons (1.8 kb and 1.9 kb) for the S segment and three overlapping amplicons (2.5 kb, 2.6 kb and 3.2 kb) for the L segment. The amplicons were purified from agarose gels and subjected to Illumina next generation sequencing. The read depth was at least 1,000,000 reads at each site in the LASV genome (S1 Fig). Alternate alleles with variation frequency above 0.1% at each position of the genomic RNA were included for analysis.

We examined the distribution and the number of variants in viral genomic RNA from mock- and 5-FU-treated samples (Fig 8 and Table). In mock samples, a total of 87 sites in ExoN- LASV genomic RNA had alternate alleles with frequencies above 0.1%, higher than the 28 sites with alternate alleles in wt rLASV genomic RNA (Table). Among the 87 sites identified in ExoN- LASV genomic RNA, 65 sites were in L gRNA (Table). The low frequency of nucleotide substitution in 5-FU samples (0.1-1%) was correlated with the low level of 5-FU treatment (100 μM). At 100 μM 5-FU, 323 sites in ExoN- LASV genomic RNA had alternate alleles (Table), substantially higher than the 104 positions identified in wt LASV RNA.

Table: NGS data of the number of sites and the variation rate of LASV genomic RNA following 5-FU treatment

	Sites with variation			Variation Rate (x10^{-5})			Relative variation Rate		
	S RNA	L RNA	S & L	S RNA	L RNA	S & L	S RNA	L RNA	S & L
Wt FU 0 μM	11	17	28	1.16	2.15	1.84	1.00	1.00	1.00
Wt FU 100 μM	67	37	104	3.41	1.68	2.22	2.93	0.78	1.21
ExoN- FU 0 μM	22	65	87	1.51	4.92	3.84	1.29	2.29	2.09
ExoN- FU 100 μM	162	161	323	8.06	7.18	7.46	6.92	3.34	4.05

wt: wild rLASV; ExoN-: ExoN- rLASV, FU: 5-FU

We further compared the nucleotide variation rate of wt- and ExoN- rLASV genomic RNA (Table). In the absence of 5-FU, the variation frequency of wt rLASV genomic RNA was 1.84 x 10^{-5} per nucleotide read. Treatment with 100 μM of 5-FU increased the variation rate of wt rLASV genomic RNA by 21% to 2.22 x 10^{-5} per nt read. For ExoN- rLASV, the variation frequency of genomic RNA was 3.84 x 10^{-5} per nt read at 0 μM 5-FU, 2.09-fold of that of wt rLASV. At 100 μM 5-FU, the variation frequency of ExoN- rLASV genomic RNA was increased by 95% to 7.46 x 10^{-5} per nt read and was 3.34-fold of the variation frequency of wt rLASV.

5-FU incorporation causes A:G and U:C transitions in viral RNA during LCMV and SARS-CoV-1 infection (43, 44). In this study, we found A:G and U:C transitions at 78 sites (75.7%) and 278 sites (86.1%) in wt rLASV genomic RNA and ExoN- rLASV genomic RNA, respectively in 5-FU samples (Fig 9). In the mock samples, A:G and U:C transition was identified at 7 sites (25%) and 32 sites (36.8%) in wt rLASV and ExoN- rLASV genomic RNA, respectively.

In summary, the NGS data indicated that lack of ExoN activity increased the frequency of single nucleotide variation in LASV genomic RNA in both mock and sublethal 5'-FU conditions.

Discussion

The LASV NP ExoN activity is known to be essential for LASV evasion of host innate immune responses. Interestingly, the DEDDh motif and the ExoN activity is highly conserved in the arenavirus family, regardless of viral pathogenicity, implying it has additional function(s) in arenavirus lifecycle. In this study, we found that abrogation of NP ExoN impaired LASV growth and RNA replication in IFN-deficient Vero cells. In addition, ExoN- rLASV was more prone to producing aberrant viral RNAs and more sensitive to mutagenic nucleoside analogues. Thus, LASV NP ExoN has a previously unrecognized function in LASV RNA replication, which reduces rates of viral RNA substitution and production of aberrant viral RNA. As the ExoN motif is highly conserved in arenaviruses, future studies should seek to determine whether the NP ExoN of other arenaviruses are also important in viral RNA replication.

In this study, we presented the evidence that abrogation of NP ExoN led to impaired LASV growth and smaller plaque size in IFN-deficient Vero cells (Fig 2). We also found that rLASV with NP D389AG392A mutation was not viable. These data demonstrated that NP ExoN is important for LASV fitness in addition to its role in immune evasion. Other groups have reported that deficiency in NP ExoN leads to attenuated growth for rMOPV, rPICV and the AV strain of rLASV (26, 27, 31). In addition, PICV possessing the NP D380A mutation (equivalent to the NP D389A mutation for LASV) forms smaller plaques in Vero cells. PICV wt revertant, which forms large plaques, could be readily identified after two passages of the NP D380A PICV mutant (27). Therefore, NP ExoN could be important for arenavirus fitness in general.

335 The present study provides evidence that abrogation of NP ExoN activity affected
336 LASV RNA replication in IFN-deficient cells (Fig 3), which explains the impaired growth
337 of ExoN- rLASV. For RNA viruses, the RNA replication is error-prone as RdRp lacks
338 proofreading activity. When nucleotide mis-incorporation occurs, RdRp may pause or
339 stop RNA elongation, which consequently affects viral RNA synthesis. Interestingly,
340 MOPV NP and LCMV NP have been shown to excise mismatched nucleotides at the 3'-
341 end of the dsRNA substrate in biochemical studies (28). Accordingly, it is plausible that
342 LASV NP ExoN could also remove mis-incorporated nucleotides like MOPV NP and
343 LCMV NP and facilitate viral RNA synthesis. In this scenario, lack of NP ExoN may
344 affect the yield or the rate of arenaviral RNA synthesis, which may partly explain the
345 impaired viral RNA replication in ExoN- rLASV infection. Further studies are required to
346 investigate whether LASV NP ExoN can excise mismatched nucleotides, through which
347 ExoN helps to reduce nucleotide mis-incorporation and facilitate viral RNA synthesis.
348 We detected increased production of aberrant S gRNA and L gRNA in ExoN- rLASV
349 infected cells in repeated experiments (Fig 4). This data indicated that loss of LASV NP
350 ExoN affected the integrity of viral genomic RNA. Sanger sequencing analysis of nearly
351 full-length S gRNA amplicons identified two types of deletion mutants in ExoN- rLASV
352 samples. Three of ten colonies had a 37-nt deletion (nt1824-1860, S agRNA) located in
353 the 67-nt-long IGR (site I to site I' shown in Fig 5A and 5B). Five colonies contained a
354 231-nt deletion (nt1616-1846 in S agRNA, from II to II' shown in Fig 5C) in the IGR and
355 NP coding region. The 37-nt deletion could disrupt the stem-loop structure in IGR,
356 meanwhile the 231-nt deletion could disrupt the IGR structure and cause a shift in open
357 reading frame from NP residue 507. In comparison, only two out of ten colonies of wt

rLASV S samples had the 37-nt deletion in IGR. As the IGR is essential for transcription termination of arenavirus mRNA and packaging of genomic RNA into progeny virus particles, abrogation of NP ExoN may indirectly affect these two important steps in viral RNA replication.

To better understand the spectrum of LASV SgRNA variants, we utilized PacBio SMRT long-read sequencing to characterize LASV SgRNA amplicon at the single-molecule level. Short-read Illumina NGS has low sensitivity and high false positive rates in solving complex Structural Variations (SVs) with deletions and insertions at least 50 nt in size (46). PacBio SMRT long-read sequencing can determine the circular consensus sequence of full-length cDNA up to 10kb long at the single-molecule level, which is ideal for analyzing RNA quasi-species, long amplicons, and SVs. In addition, SMRT long-read technology is suitable for sequencing through highly repetitive, GC-rich sequences that are present in the IGRs of arenavirus RNA. In this study, raw reads with a minimum number of 3 passes and higher than 99% accuracy were used to generate the CCS reads to ensure read accuracy. The mean number of read passes for each cDNA was 28 times for wt rLASV with an average read length of 2319 nt, and 26 times for ExoN- rLASV with an average read length of 2610 nt (Fig 6A). The mean reading score of the SMRT assay was >99.9%. Variants with >3% frequency was selected in data analysis to ensure the reliability of the reads. The results demonstrated that 88.9% and 4.9% of the S genomic RNA contained the 231-nt deletion and the 37-nt deletion in ExoN- rLASV sample, respectively. In comparison, 7.1% and 18.2% of the S RNA in wt rLASV sample has the 231-nt deletion and the 37-nt deletion, respectively. In addition, higher than 99.93% of ExoN- rLASV S gRNA harbored the intended NP D389A

mutation, which confirmed that the NP D389A mutation was maintained in ExoN- rLASV. Our data suggests that NP ExoN is important for viral control of structural deletion in LASV genomic RNA.

The molecular basis for these structural deletions formed in ExoN- rLASV S RNA is unclear. Sequence analysis revealed the presence of homologous sequences flanking the 37-nt deletion and the 231-nt deletion in S RNA (Fig 10, boxed sequences, sites I/I' for the 37-nt deletion, sites II/II' for the 231-nt deletion). Based on the homologous sequences, we propose a stop-and-realign model for the mechanism of increased structural deletions in S RNA in ExoN- rLASV infection (Fig 10). When RNA synthesis error occurs, LASV NP ExoN may excise the mismatched nucleotide, like its MOPV and LCMV counterparts (28), and allows the RdRp to resume RNA elongation. Lack of NP ExoN activity may lead to the stop of viral RNA synthesis, as shown in Fig 10A for the 37nt-deletion and in Fig 10B for the 231nt-deletion (Step 1, mis-incorporation and stop). Depending on the nucleotide mis-incorporated, LASV RdRp L protein may realign the 3'-end of nascent RNA (at site I in Fig 10A and site II in Fig 10B) with downstream homologous sequences on the template RNA (sites I' and II' in Fig 10A and Fig 10B, respectively) and resume RNA elongation (Step 2, realign and resume). As a result, RdRp skips the regions between these homologous sequences, leading to the 37-nt deletion (Fig 10A) and the 231-nt deletion (Fig 10B) in S RNA, respectively. Thus, LASV NP ExoN may control structural deletions by reducing errors in LASV RNA synthesis. In this regard, it is worth noting that RNA viruses with low-fidelity RdRp, such as Sindbis virus or tombusvirus, exhibit an increased production of defective viral genomic RNA correlated with an enhanced rate of viral RNA recombination (47-49). Further studies

404 are warranted to investigate the molecular basis of increased aberrant RNA formation
405 associated with LASV NP ExoN deficiency and the impact on virus infection.

406 Our data of nucleoside analogue study support that LASV NP ExoN contributes to
407 control the frequency of nucleotide substitution in viral RNA. In LCMV infection, 5-FU
408 could be incorporated into nascent viral RNA and cause mutations that affect virus
409 fitness. Consistently, abrogation of NP ExoN rendered LASV more sensitive to the
410 mutagenic nucleoside analogues 5-FU and EIDD-1931 in virus titration assay (Fig 7).
411 Our NGS data showed that ExoN deficiency is associated with increased nucleotide
412 substitution in rLASV RNA following 5-FU treatment. At 100 μM 5-FU, the mutation rate
413 of ExoN- rLASV was increased by 94%, while that of wt rLASV was increased by 21%.
414 In the absence of 5-FU, the variation frequency of ExoN- rLASV genomic RNA was
415 2.09-fold of that of wt rLASV, suggesting LASV NP ExoN controls RNA substitution
416 under normal culture conditions. Of note, 5-FU-associated A:G and U:C transitions
417 accounted for 75.7% or 86.1% of the alternate alleles identified in wt or ExoN- rLASV
418 genomic RNA, respectively, following 5-FU treatment (Fig 9). This data confirmed that
419 the nucleotide substitution in 5-FU samples (Fig 7) was largely related to 5-FU
420 incorporation.

421 For RNA virus, the error-prone RNA replication could increase genetic diversity in
422 virus population and provide benefits for adaptation. However, the mutation rate has to
423 be controlled as even a moderate 1.1-2.8-fold increase in mutation rate could drastically
424 affect virus fitness (50). As negative-sense RNA viruses, how arenaviruses balance the
425 mutation rate while preserving fidelity is largely unknown. Our nucleotide analogue data
426 indicated that LASV NP ExoN contributes to control the rate of viral RNA substitution

and ensure the fidelity of viral RNA synthesis. To the best of our knowledge, this is the first example among negative-sense RNA viruses that a non-RdRp viral protein plays a key role in viral RNA fidelity.

In summary, the present study provided evidence that LASV NP ExoN is required for optimal viral RNA replication and mutation control in addition to its role in immune evasion. Loss of LASV NP ExoN activity has multiple impacts on viral RNA replication, including decreased RNA level, increased occurrence of structural deletions in viral RNA, and higher rate of nucleotide substitution. These defects may have more profound impact on viral fitness and pathogenicity *in vivo*. Future studies are warranted to investigate whether NP ExoN of other arenaviruses has similar functions in viral RNA replication. Hemorrhagic fever-causing arenaviruses continue to pose a threat to public health and have pandemic potential. Currently, mutagenic nucleotide analogue T705 (Favipiravir) shows promising activities in animal models of arenavirus infection (51, 52). Our study suggests that targeting NP ExoN may enhance virus sensitivity to nucleotide analogues. Therefore, developing NP ExoN inhibitors could be a valuable strategy to enhance the efficacy of T705 in treatment of LF and other arenavirus-caused hemorrhagic fever diseases.

Materials and Methods

Cells and Viruses.

Vero cells (CCL-81, ATCC) were maintained in Dulbecco's modified eagle medium (Hyclone) supplemented with 10% FBS (Invitrogen) and 1% penicillin and streptomycin solution (Hyclone). The LASV (Josiah strain) used in studies was recombinant virus that

were rescued using reverse genetic systems in BHK21 cells and passaged only once (P1) in Vero cells as previously described (53). All plasmids used for LASV rescue were confirmed by sequencing. Site-directed mutagenesis on the pmPol I-LASV Sag plasmid was performed using QuikChange II kit (Agilent) according to the manufacturer's instructions. To construct the rLASV NPD380A mutant, forward primer 5'-CCAAATGCT AAGACCTGGATGGCTATTGAAGGAAGACCTGAAGATC-OH, and reverse primer 5'-GATCTTCAG GTCTTCCTTCAATAGCCATCCAGGTCTTAGCATTTGG-OH were used. To construct the rLASV NP D389AG392A mutant, forward primer 5'-AAATGCTAAGAC CTGGATGGCTATTGAAGCTAGACCTGAAGATCCAGTGG-OH, and reverse primer 5'-CCACTGGATCTTCAGGTCTAGCTTCAATA GCCATCCAGGTCTTAGCATTT-OH were used. The sequence of mutant rLASV was confirmed by Sanger Sequencing after RT-PCR amplification of viral RNA extracted from infected cells. All infection work with pathogenic arenaviruses was performed at the BSL4 facilities in Galveston National Laboratory in the University of Texas Medical Branch in accordance with institutional health and safety guidelines and federal regulations.

RNA Extraction, RT-PCR, and real-time RT-qPCR

RNA lysates were prepared using the TRIzol reagent (Life Technology). RNA was purified using the RNeasy Minikit (Qiagen) and treated with DNase I (Qiagen) as previously reported (32, 54). An equal amount of total RNA (0.5 to 1µg) was reverse transcribed to cDNA at 55 ^{o}C for 60 minutes using high-fidelity reverse transcriptase SuperScript IV (Invitrogen) per manufacturer's instruction. The high-fidelity reverse transcriptase SuperScript IV has low RNase H activity and is suitable for long cDNA synthesis. Random hexamer primers and sequence specific primers were used in RT as

specified in each experiment. cDNA samples were treated with RNase H. In RT of S gRNA, an S gRNA 3'UTR specific primer (5'-CGCACAGTGGATCCTAGGCTA-OH) was used. In RT of L gRNA, an L gRNA 3'UTR specific primer (5'- CACCGAGGATCCTAGG CATTAAGGCTATC-OH) was used in cDNA synthesis. PCR amplification of close to full-length Sg cDNA (3391bp) was conducted with Platinum SuperFi DNA Polymerase (Invitrogen) using forward primer 5'-ATCCTAGGCATTTTTGGTTGC-OH and reverse primer 5'-CGCACAGTGGATCCTAGGCTA-OH. PCR amplification of close to full-length Lg cDNA (7265 bp) was performed with Platinum SuperFi DNA Polymerase using forward primer 5'-CACCGAGGATCCTAGG CATTAAGGCTATC-OH and reverse primer 5'-ATCCTAGGCAATTTGGTTGTTCTTTTTTGAG-OH. Real-time quantitative PCR (qPCR) was performed with SsoAdvanced Universal SYBR green Supermix (BioRad) on a CFX96 real-time PCR detection system (BioRad) as described previously (32, 54). To measure the viral RNA level at NP locus and L locus, cDNA synthesized with random primers was used in a qPCR assay. LASV NP forward primer (5′-GAAGGGCCT GGGAAAACACT-OH) and LASV NP reverse primer (5′-AGGTAAGCCCAGCGGTAAA C-OH) were used for the NP locus. LASV L forward primer (5′-CAGCAGGTCAGACGA AGTGT-OH) and LASV L reverse primer (5′-GTTGTGCATAGGGGAGGCTT-OH) were used for the L locus. The cDNA synthesized with SgRNA- and LgRNA-specific primers as indicated above was used in a qPCR assay to measure the level of LASV Sg RNA and Lg RNA. The qPCR data was analyzed with the CFX Manager software (BioRad). The RNA level of each target gene was normalized to that of the housekeeping gene β-actin with validated primers from BioRad. All experiments were performed separately in triplicates.

PacBio SMRT long-read sequencing of LASV SgRNA

Vero cells was infected by ExoN- rLASV and wt rLASV at a MOI of 1. At 48 hpi, total RNA was purified from infected cells. RT-PCR amplification of the close-to-full-length SgRNA was performed as described above. PCR amplicons (approximately 3.4 kb) were gel purified using Monarch DNA gel extraction kit (NEB). Library construction, PacBio SMRT long-read sequencing and CCS determination was performed by Azenta Life Sciences (USA). At least 1 µg of amplicon was ligated to barcoded adapters (Pacific Biosciences) for SMRTbell library construction and then sequenced on the PacBio Sequel IIe platform with v3.0 chemistry. Raw reads with a minimum number of passes greater than 3 were used to generate the CCS reads using PacBio SMRTLINK v.10.1. HiFi reads (>=99% accuracy) were extracted. Data analysis was performed utilizing *Galaxy*: an open source, web-based platform supported by NIH, NSF, and the Texas Advanced Computing Center. CCS reads were filtered for those with size 3100-3394bp and high-quality reads (Phred>20) using Filter FASTQ and mapped to the LASV reference seq (MH358389) with *Minimap2* (PacBio HiFi reads vs reference mapping (-k19 -w19 -U50,500 -g10k -A1 -B4 -O6,26 -E2,1 -s200)). Variants with cutoff >3% frequency were called with *iVar* and visualized using the Integrated Genomics Viewer (IGV). The raw sequencing data has been deposited in Sequence Read Archive (SRA) databases hosted by the National Library of Medicine's National Center for Biotechnology Information (NCBI), NIH.

Mutagenic nucleotide analogue treatment

5-fluorouracil (Cat# 03738, Sigma) and N4-hydroxycytidine (EIDD-1931) (Cat#9002958, Cayman) were dissolved in DMSO (cell culture grade, Sigma) and further diluted in

519 DMEM media contain 2% FBS and 0.1% DMSO. Vero cells were mock-treated or
520 treated with 5-FU or EIDD-1931 at different concentrations as indicated in each
521 experiment for 4 hr and then infected with wt rLASV and ExoN- rLASV at a MOI of 0.1
522 for 1 hr. Virus inoculums were removed and replaced with fresh media (DMEM + 2%
523 FBS and 0.1% DMSO) containing 5-FU or EIDD-1931 of different concentrations as
524 indicated. At 48 hpi, the supernatants of infected cells were harvested and subjected to
525 plaque assay to determine virus titers. The viability of Vero cells treated with 5-FU and
526 EIDD-1931 alone were assessed using CellTiter-Glo Viability Assay (Promega).

527 **Illumina NGS analysis of LASV RNA amplicons following 5-FU treatment.**

528 Virus infection and 5-FU treatment of Vero cells were performed as described above.
529 The supernatants of virus infected cultures were harvested and clarified by
530 centrifugation at 3,000 rpm to remove cell debris. Virions were concentrated and
531 purified with Amicon Ultra-15 Centrifugal Filter Units (Millipore, MW cutoff 100 kD). RNA
532 extraction and reverse transcription with S gRNA and L gRNA-specific primers were
533 performed as described above. PCR were performed with high-fidelity Platinum SuperFi
534 DNA Polymerase. For S gRNA, two overlapping amplicons were amplified. For L gRNA,
535 three overlapping amplicons were amplified. The primers used in amplicon preparation
536 are listed in supplementary information (S2 Table). All amplicons were purified from
537 agarose gel after electrophoresis. Library construction, Illumina deep sequencing
538 (Hiseq, 2x150 bp, pair-end) and raw data process was performed by Azenta Life
539 Sciences (USA). The obtained reads had a mean read quality score over 37. More than
540 90% of the bases had a Phred quality score greater that 30 (i.e., sequencing accuracy
541 of 99.9%). Data processing and analysis was performed on *Galaxy*, a web-based

platform supported by NIH, NSF, and the Texas Advanced Computing Center. The raw data (in FASTQ format) was trimmed with *Trimmomatic* (55) to remove adaptor sequences, and then mapped to the LASV reference seq (MH358389) with minimap2 (41) (short reads without splicing (-k21 -w11 --sr -F800 -A2 -B8 -O12,32 -E2,1 -r50 -p.5 -N20 -f1000,5000 -n2 -m20 -s40 -g200 -2K50m --heap-sort=yes --secondary=no). Read depth was assessed with Samtools (56). The read depth was higher than 1,000,000 reads at each site on LASV genomic RNA, except for some positions at IGR. Low frequency variants were called with LoFreq (57) (minimal base calling quality>20 for reference bases and alternate bases, minimum mapping quality 20) from one million reads at each position. Single nucleotide variations with higher than 0.1% frequency was included for analysis to minimize background noise due to sequencing error. To ensure the confidence of data quality, reads with strand bias greater than 100 (SB>100) were excluded. The data were imported to Excel for mutation analysis. Raw NGS data have been deposited in SRA databases hosted by NCBI, NIH.

Acknowledgments

This work was supported in part by Public Health Service grants 1R21AI166985 (to CH) R01AI093445 (to SP) and R01AI129198 (to SP). CH was also supported by Institute for Human Infections & Immunity, UTMB Pilot Study Fund (P86035) and would like to acknowledge Galveston National Laboratory (supported by the Public Health Service award 5UC7AI094660) for support of research activity. Research work in Dr. Paessler's lab was also supported by the John. S. Dunn Distinguished Chair in Biodefense

564 endowment. E.K.M was supported by National Institutes of Health T32 training grant
565 AI060549.

566

567

Figure legends

Figure 1. (A). Schematic diagram of arenavirus S and L genomic RNA. On each genomic RNA, an Intergenic Region (IGR) separates two ORFs. The highly structured IGRs are the termination signals of viral mRNA transcription and are required for efficient packaging of viral genomic RNA into progeny virions. **(B).** Genomic RNA replication and mRNA transcription of arenavirus S RNA. After virus entry, L protein and NP transcribe NP mRNA from S gRNA. From S gRNA, S antigenomic RNA (S agRNA) is also synthesized, which is the template for GPC mRNA and S gRNA synthesis later in virus infection. Arenavirus mRNA lacks a poly-A tail and contains the structured IGR at the 3'-end.

Figure 2. Abrogation of NP ExoN activity impaired LASV multiplication in interferon-deficient cells.

A recombinant LASV (rLASV) with NP D389A mutation was rescued (ExoN- rLASV). (**A**). The D389A mutation was maintained after 3 passages in Vero cells (Sanger sequencing). (**B**). The growth curve of wild-type rLASV (wt) and the ExoN- rLASV (NP ExoN-) in Vero cells at multiplicity of infection (MOI) 0.01 and MOI 1. Dashed lines denote the detection limit of plaque assay. (**C**) The plaque morphology of wt rLASV (wt) and ExoN- rLASV.

Figure 3. Abrogation of NP ExoN activity affected LASV RNA replication.

Vero cells were infected with wt rLASV and ExoN- rLASV (MOI=0.01 and 1.0). At 72 hpi (MOI 0.01) or 24 hpi (MOI 1.0), virus titer was determined by plaque assay **(A)**. RT-

591 qPCR assay for viral RNA level at the NP locus **(B)** and L locus **(C)**. The viral RNA level
592 for S gRNA **(D)** and L gRNA **(E)** were also determined by qRT-PCR. The viral RNA level
593 was normalized to the level of host β-actin mRNA and are presented as the fold
594 changes relative to the level of ExoN- rLASV samples (set as 1.0). The data presents
595 the mean and SEM of three independent experiments. (*: P<0.01; **: P<0.02; ***:
596 P<0.05 with Student *t*-test).

597 **Figure 4. Aberrant viral RNA formation in ExoN- rLASV infection**

598 Vero cells were infected with wt rLASV (wt) and ExoN- rLASV (ExoN-) at MOI 0.01 for
599 72 hr and at MOI 1 for 24 hr. RNA samples were purified from infected cells and
600 transcribed to cDNA with primers targeting the 3'-end of S gRNA and L gRNA,
601 respectively. High-fidelity PCR was performed to amplify close-to-full-length S gRNA
602 (3391 nt) and L gRNA (7265 nt) followed by agarose gel electrophoresis. (**A**). RT-PCR
603 result of S gRNA (S). S' is a slightly fast-migrating aberrant S RNA product in ExoN-
604 rLASV samples. (**B**). RT- PCR result of L gRNA. Several aberrant L gRNA products in
605 ExoN- rLASV samples (3.5 kb to 6 kb) are observed. The aberrant RNA products are
606 indicated by asterisk (*). Plasmid: PCR product using a plasmid containing LASV L
607 segment as template.

608 **Figure 5. Sanger sequencing of aberrant S RNA formed in ExoN- rLASV infection.**
609 **(A)**. Predicted RNA structure of IGR of S RNA by *mFold.* **(B).** In ExoN- rLASV, a 37-nt
610 deletion (nt1824-1860 in S agRNA) from site I to site I' disrupted IGR structure. **(C)** a
611 231-nt deletion (nt1616-1846 in S agRNA) from the C-terminus of NP at site II' to site II
612 in the IGR (refer to A) was identified in the S gRNA sample of ExoN- rLASV.

613 **Figure 6. PacBio SMRT long-read sequencing of S gRNA in rLASV samples.**

Vero cells were infected with wt rLASV and ExoN- rLASV (MOI 1.0). RT-PCR product of the close-to-full-length SgRNA (3391 nt) were purified after agarose gel electrophoresis and subjected to PacBio SMRT long-read sequencing (Sequel IIe) with v3.0 chemistry. **(A).** HiFi CCS reads were generated using PacBio SMRTLINK v.10.1. **(B).** CCS reads with size 3100-3391bp were selected with Filter FASTQ and mapped to LASV reference seq (GenBank MH358389) with *minimap2.* Variants were called with *ivar* and visualized using Integrated Genomics Viewer. **(C)**. The percentage of the 231-nt deletion and the 37-nt deletion in S RNA of wt rLASV and ExoN- rLASV sample.

Figure 7. NP ExoN deficiency enhanced LASV sensitivity to mutagenic nucleotide analogues.

(A). Vero cells were treated with 5'-FU and EIDD-1931 at indicated concentrations. At 48 hr post treatment, cell viability was measured using CellTiter-Glo Viability Assay (Promega). Data shown are the average (n=4) and SEM. **(B) and (C).** Vero cells were treated with 5-FU and EIDD-1931 at different concentrations as indicated. Cells were infected with wt rLASV (wt) and ExoN- rLASV (ExoN-) at MOI 0.1. At 48 hpi, virus titers were determined by plaque assay. Log10 virus titer changes relative to the virus titer of non-treated cells are shown. Data presented are the mean and the SEM of three independent experiments.

Figure 8. Distribution of alternate alleles in LASV genomic RNA following 5-FU treatment

Vero cells were mock-treated or treated with 5-FU and infected with wt rLASV and ExoN- rLASV (MOI 0.1). The distribution of alternate alleles in LASV S segment RNA **(A)** and L segment RNA **(B)** are shown. Y axis shows the frequency of variations on

637 each position of viral genomic RNA. X axis shows the genomic position of LASV
638 agRNA.

639 **Fig 9: The number of positions with base changes in viral genomic RNA.**

640 All values represent the number of positions with alternate alleles at frequency higher
641 than 0.1% in wt rLASV and ExoN- rLASV genomic RNA following 0 μM and 100 μM 5-
642 FU treatment. Base transitions (A:G, G:A, U:C and C:U) are shaded in grey. 5-FU
643 specific transitions (A:G and U:C) are marked with asterisk. Base transversions
644 between purines and pyrimidines are shown in white.

645 **Figure 10. A stop-and-realign model for the 37-nt deletion (A) and the 231-nt**
646 **deletion (B) in S RNA of ExoN- rLASV**.

647 Homologous sequences flanking the deletion sites are indicated as boxed sequences
648 (sites I/I' for the 37-nt deletion, sites II/II' for the 231-nt deletion). Sites I and II are
649 located in IGR stem-loop structure. In viral RNA synthesis, NP ExoN may remove mis-
650 incorporated nucleotide and helps LASV RdRp L protein to resume viral RNA
651 elongation. In the absence of NP ExoN, viral RNA elongation may terminate (Step 1).
652 Depending on the nucleotide mis-incorporated (i.e., an A instead of C as shown in A
653 and B), viral RdRp L protein may realign the 3'-end of nascent RNA (5'-CCGUGACA in
654 site I or 5'-GUGACA in site II) with downstream homologous sequences on the template
655 RNA (3'-GGGACUGU-5' in site I' and 3'-CACCGU-5' in site II') and resume RNA
656 elongation (Step 2). Thus, the 37-nt deletion and the 231-nt deletion in S RNA may
657 result from viral RdRp skipping the regions between the homologous sequences, an
658 error that could be controlled by functional NP ExoN.

659

Supporting information

S1 Fig: Read depth of viral genomic RNA in NGS analysis.

S2 Table: Primers used in PCR amplification of LASV amplicon for NGS analysis.

References

1. Maes P, Adkins S, Alkhovsky SV, Avsic-Zupanc T, Ballinger MJ, Bente DA, et al. Taxonomy of the order Bunyavirales: second update 2018. Arch Virol. 2019;164(3):927-941.
2. Shi M, Lin XD, Chen X, Tian JH, Chen LJ, Li K, et al. The evolutionary history of vertebrate RNA viruses. Nature. 2018;556(7700):197-202.
3. Geisbert TW, Jahrling PB. Exotic emerging viral diseases: progress and challenges. Nature medicine. 2004;10(12 Suppl):S110-121.
4. Gunther S, Lenz O. Lassa virus. Critical reviews in clinical laboratory sciences. 2004;41(4):339-390.
5. McCormick JB, Webb PA, Krebs JW, Johnson KM, Smith ES. A prospective study of the epidemiology and ecology of Lassa fever. J Infect Dis. 1987;155(3):437-444.
6. Dan-Nwafor CC, Furuse Y, Ilori EA, Ipadeola O, Akabike KO, Ahumibe A, et al. Measures to control protracted large Lassa fever outbreak in Nigeria, 1 January to 28 April 2019. Euro Surveill. 2019;24(20).
7. Gomez RM, Jaquenod de Giusti C, Sanchez Vallduvi MM, Frik J, Ferrer MF, Schattner M. Junin virus. A XXI century update. Microbes and infection. 2011;13(4):303-311.

683 8. Grant A, Seregin A, Huang C, Kolokoltsova O, Brasier A, Peters C, et al. Junin virus
684 pathogenesis and virus replication. Viruses. 2012;4(10):2317-2339.
685 9. Patterson M, Grant A, Paessler S. Epidemiology and pathogenesis of Bolivian
686 hemorrhagic fever. Curr Opin Virol. 2014;5:82-90.
687 10. Sarute N, Ross SR. New World Arenavirus Biology. Annu Rev Virol. 2017;4(1):141-
688 158.
689 11. Gunther S, Lenz O. Lassa Virus. Critical Reviews in Clinical Laboratory
690 Science2004. p. 339-390.
691 12. Lukashevich IS. Advanced vaccine candidates for Lassa fever. Viruses.
692 2012;4(11):2514-2557.
693 13. Sattler RA, Paessler S, Ly H, Huang C. Animal Models of Lassa Fever. Pathogens.
694 2020;9(3).
695 14. World Health Organization. 2018 Annual review of diseases prioritized under the
696 Research and Development Blueprint 2018 [Available from:
697 http://www.who.int/blueprint/priority-diseases/en/.
698 15. Buchmeier MJ, de la Torre JC, Peters CJ. Arenaviridae: the viruses and their
699 replication. 5th ed. Knipe DM, PM H, editors. Philadelphia, PA, USA: Wolter Kluwer
700 Lippincott Williams & Wilkins; 2007. 1791–1827 p.
701 16. Pinschewer DD, Perez M, de la Torre JC. Dual role of the lymphocytic
702 choriomeningitis virus intergenic region in transcription termination and virus
703 propagation. J Virol. 2005;79(7):4519-4526.

17. Pinschewer DD, Perez M, de la Torre JC. Role of the virus nucleoprotein in the regulation of lymphocytic choriomeningitis virus transcription and RNA replication. J Virol. 2003;77(6):3882-3887.
18. Pyle JD, Whelan SPJ. Isolation of Reconstructed Functional Ribonucleoprotein Complexes of Machupo Virus. J Virol. 2021;95(22):e0105421.
19. Baird NL, York J, Nunberg JH. Arenavirus infection induces discrete cytosolic structures for RNA replication. J Virol. 2012;86(20):11301-11310.
20. Hastie KM, Liu T, Li S, King LB, Ngo N, Zandonatti MA, et al. Crystal structure of the Lassa virus nucleoprotein-RNA complex reveals a gating mechanism for RNA binding. Proc Natl Acad Sci U S A. 2011;108(48):19365-19370.
21. Hastie KM, Kimberlin CR, Zandonatti MA, MacRae IJ, Saphire EO. Structure of the Lassa virus nucleoprotein reveals a dsRNA-specific 3' to 5' exonuclease activity essential for immune suppression. Proc Natl Acad Sci U S A. 2011;108(6):2396-2401.
22. Jiang X, Huang Q, Wang W, Dong H, Ly H, Liang Y, et al. Structures of arenaviral nucleoproteins with triphosphate dsRNA reveal a unique mechanism of immune suppression. J Biol Chem. 2013;288(23):16949-16959.
23. Qi X, Lan S, Wang W, Schelde LM, Dong H, Wallat GD, et al. Cap binding and immune evasion revealed by Lassa nucleoprotein structure. Nature. 2010;468(7325):779-783.
24. Mantlo E, Paessler S, Huang C. Differential Immune Responses to Hemorrhagic Fever-Causing Arenaviruses. Vaccines (Basel). 2019;7(4).

726 25. Meyer B, Ly H. Inhibition of Innate Immune Responses Is Key to Pathogenesis by
727 Arenaviruses. J Virol. 2016;90(8):3810-3818.
728 26. Carnec X, Mateo M, Page A, Reynard S, Hortion J, Picard C, et al. A Vaccine
729 Platform against Arenaviruses Based on a Recombinant Hyperattenuated Mopeia
730 Virus Expressing Heterologous Glycoproteins. J Virol. 2018;92(12):J Virol
731 92:e0223017. https://doi.org/0223010.0221128/JVI.0202230-0223017.
732 27. Huang Q, Shao J, Lan S, Zhou Y, Xing J, Dong C, et al. In vitro and in vivo
733 characterizations of pichinde viral nucleoprotein exoribonuclease functions. J Virol.
734 2015;89(13):6595-6607.
735 28. Yekwa E, Aphibanthammakit C, Carnec X, Coutard B, Picard C, Canard B, et al.
736 Arenaviridae exoribonuclease presents genomic RNA edition capacity. bioRxiv.
737 2019:541698.
738 29. Groseth A, Hoenen T, Weber M, Wolff S, Herwig A, Kaufmann A, et al. Tacaribe
739 virus but not junin virus infection induces cytokine release from primary human
740 monocytes and macrophages. PLoS Negl Trop Dis. 2011;5(5):e1137.
741 30. Pannetier D, Faure C, Georges-Courbot MC, Deubel V, Baize S. Human
742 macrophages, but not dendritic cells, are activated and produce alpha/beta
743 interferons in response to Mopeia virus infection. J Virol. 2004;78(19):10516-10524.
744 31. Carnec X, Baize S, Reynard S, Diancourt L, Caro V, Tordo N, et al. Lassa virus
745 nucleoprotein mutants generated by reverse genetics induce a robust type I
746 interferon response in human dendritic cells and macrophages. J Virol.
747 2011;85(22):12093-12097.

748 32. Mateer EJ, Maruyama J, Card GE, Paessler S, Huang C. Lassa Virus, but Not
749 Highly Pathogenic New World Arenaviruses, Restricts Immunostimulatory Double-
750 Stranded RNA Accumulation during Infection. J Virol. 2020;94(9):e02006-02019.
751 https://doi.org/02010.01128/JVI.02006-02019.
752 33. Denison MR, Graham RL, Donaldson EF, Eckerle LD, Baric RS. Coronaviruses: an
753 RNA proofreading machine regulates replication fidelity and diversity. RNA Biol.
754 2011;8(2):270-279.
755 34. Minskaia E, Hertzig T, Gorbalenya AE, Campanacci V, Cambillau C, Canard B, et
756 al. Discovery of an RNA virus 3'->5' exoribonuclease that is critically involved in
757 coronavirus RNA synthesis. Proc Natl Acad Sci U S A. 2006;103(13):5108-5113.
758 35. Ogando NS, Ferron F, Decroly E, Canard B, Posthuma CC, Snijder EJ. The
759 Curious Case of the Nidovirus Exoribonuclease: Its Role in RNA Synthesis and
760 Replication Fidelity. Front Microbiol. 2019;10:1813.
761 36. Osada N, Kohara A, Yamaji T, Hirayama N, Kasai F, Sekizuka T, et al. The genome
762 landscape of the african green monkey kidney-derived vero cell line. DNA Res.
763 2014;21(6):673-683.
764 37. Desmyter J, Melnick JL, Rawls WE. Defectiveness of interferon production and of
765 rubella virus interference in a line of African green monkey kidney cells (Vero). J
766 Virol. 1968;2(10):955-961.
767 38. Rhoads A, Au KF. PacBio Sequencing and Its Applications. Genomics Proteomics
768 Bioinformatics. 2015;13(5):278-289.

769 39. Lui WY, Yuen CK, Li C, Wong WM, Lui PY, Lin CH, et al. SMRT sequencing
770 revealed the diversity and characteristics of defective interfering RNAs in influenza
771 A (H7N9) virus infection. Emerg Microbes Infect. 2019;8(1):662-674.
772 40. Yamashita T, Takeda H, Takai A, Arasawa S, Nakamura F, Mashimo Y, et al.
773 Single-molecular real-time deep sequencing reveals the dynamics of multi-drug
774 resistant haplotypes and structural variations in the hepatitis C virus genome.
775 Scientific reports. 2020;10(1):2651.
776 41. Li H. Minimap2: pairwise alignment for nucleotide sequences. Bioinformatics.
777 2018;34(18):3094-3100.
778 42. Grubaugh ND, Gangavarapu K, Quick J, Matteson NL, De Jesus JG, Main BJ, et al.
779 An amplicon-based sequencing framework for accurately measuring intrahost virus
780 diversity using PrimalSeq and iVar. Genome Biology. 2019;20(1):8.
781 43. Smith EC, Blanc H, Surdel MC, Vignuzzi M, Denison MR. Coronaviruses lacking
782 exoribonuclease activity are susceptible to lethal mutagenesis: evidence for
783 proofreading and potential therapeutics. PLoS Pathog. 2013;9(8):e1003565.
784 44. Ruiz-Jarabo CM, Ly C, Domingo E, de la Torre JC. Lethal mutagenesis of the
785 prototypic arenavirus lymphocytic choriomeningitis virus (LCMV). Virology.
786 2003;308(1):37-47.
787 45. Agostini ML, Pruijssers AJ, Chappell JD, Gribble J, Lu X, Andres EL, et al. Small-
788 Molecule Antiviral beta-d-N(4)-Hydroxycytidine Inhibits a Proofreading-Intact
789 Coronavirus with a High Genetic Barrier to Resistance. J Virol.
790 2019;93(24):e01348-01319. https://doi.org/01310.01128/JVI.01348-01319.

791 46. Sedlazeck FJ, Rescheneder P, Smolka M, Fang H, Nattestad M, von Haeseler A, et
792 al. Accurate detection of complex structural variations using single-molecule
793 sequencing. Nat Methods. 2018;15(6):461-468.
794 47. Panaviene Z, Nagy PD. Mutations in the RNA-binding domains of tombusvirus
795 replicase proteins affect RNA recombination in vivo. Virology. 2003;317(2):359-372.
796 48. Poirier EZ, Mounce BC, Rozen-Gagnon K, Hooikaas PJ, Stapleford KA, Moratorio
797 G, et al. Low-Fidelity Polymerases of Alphaviruses Recombine at Higher Rates To
798 Overproduce Defective Interfering Particles. J Virol. 2015;90(5):2446-2454.
799 49. Vignuzzi M, Lopez CB. Defective viral genomes are key drivers of the virus-host
800 interaction. Nat Microbiol. 2019;4(7):1075-1087.
801 50. Holland JJ, Domingo E, de la Torre JC, Steinhauer DA. Mutation frequencies at
802 defined single codon sites in vesicular stomatitis virus and poliovirus can be
803 increased only slightly by chemical mutagenesis. J Virol. 1990;64(8):3960-3962.
804 51. Safronetz D, Rosenke K, Westover JB, Martellaro C, Okumura A, Furuta Y, et al.
805 The broad-spectrum antiviral favipiravir protects guinea pigs from lethal Lassa virus
806 infection post-disease onset. Scientific reports. 2015;5:14775.
807 52. Mendenhall M, Russell A, Smee DF, Hall JO, Skirpstunas R, Furuta Y, et al.
808 Effective oral favipiravir (T-705) therapy initiated after the onset of clinical disease in
809 a model of arenavirus hemorrhagic Fever. PLoS Negl Trop Dis. 2011;5(10):e1342.
810 53. Yun NE, Seregin AV, Walker DH, Popov VL, Walker AG, Smith JN, et al. Mice
811 lacking functional STAT1 are highly susceptible to lethal infection with Lassa virus.
812 J Virol. 2013;87(19):10908-10911.

54. Huang C, Kolokoltsova OA, Mateer EJ, Koma T, Paessler S. Highly Pathogenic New World Arenavirus Infection Activates the Pattern Recognition Receptor Protein Kinase R without Attenuating Virus Replication in Human Cells. J Virol. 2017;91(20):e01090-01017. https://doi.org/01010.01128/JVI.01090-01017.

55. Bolger AM, Lohse M, Usadel B. Trimmomatic: a flexible trimmer for Illumina sequence data. Bioinformatics. 2014;30(15):2114-2120.

56. Danecek P, Bonfield JK, Liddle J, Marshall J, Ohan V, Pollard MO, et al. Twelve years of SAMtools and BCFtools. GigaScience. 2021;10(2).

57. Wilm A, Aw PPK, Bertrand D, Yeo GHT, Ong SH, Wong CH, et al. LoFreq: a sequence-quality aware, ultra-sensitive variant caller for uncovering cell-population heterogeneity from high-throughput sequencing datasets. Nucleic Acids Research. 2012;40(22):11189-11201.

Fig 1

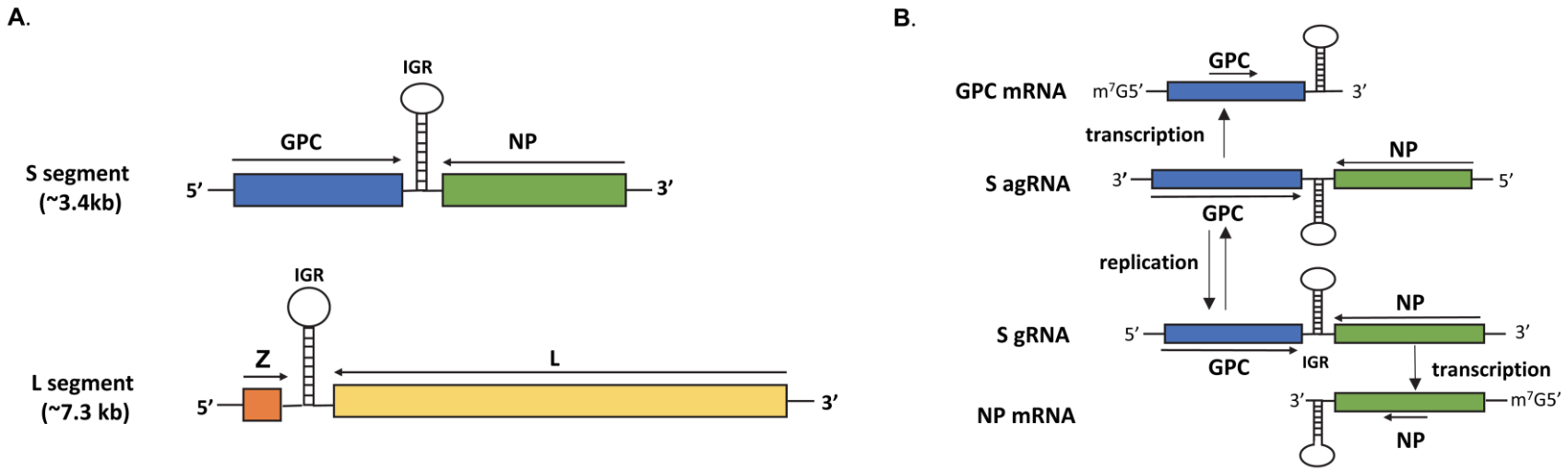
A.
S segment
(~3.4kb)
IGR
GPC
NP
5′
3′
L segment
(~7.3 kb)
IGR
Z
L
5′
3′
B.
GPC mRNA
m7G5′
GPC
3′
transcription
S agRNA
NP
3′
5′
GPC
replication
S gRNA
NP
5′
3′
GPC
IGR
transcription
NP mRNA
3′
m7G5′
NP

Fig 2

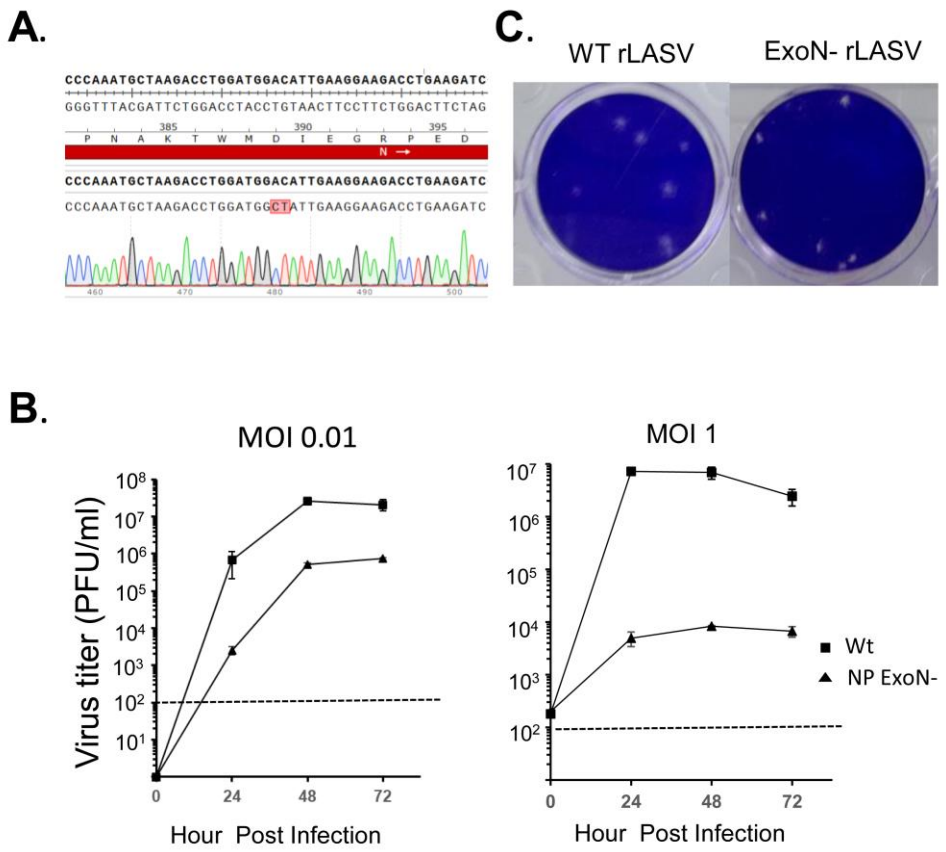
A.
CCCAAATGCTAAGACCTGGATGGACATTGAAGGAAGACCTGAAGATC
GGGTTTACGATTCTGGACCTACCTGTAACTTCCTTCTGGACTTCTAG
385
390
395
P N A K T W M D I E G R P E D
N
CCCAAATGCTAAGACCTGGATGGACATTGAAGGAAGACCTGAAGATC
CCCAAATGCTAAGACCTGGATGGCTATTGAAGGAAGACCTGAAGATC
460
470
480
490
500
C.
WT rLASV
ExoN- rLASV
B.
MOI 0.01
MOI 1
Virus titer (PFU/ml)
10^8
10^7
10^6
10^5
10^4
10^3
10^2
10^1
0
24
48
72
Hour Post Infection
Wt
NP ExoN-

Fig 3

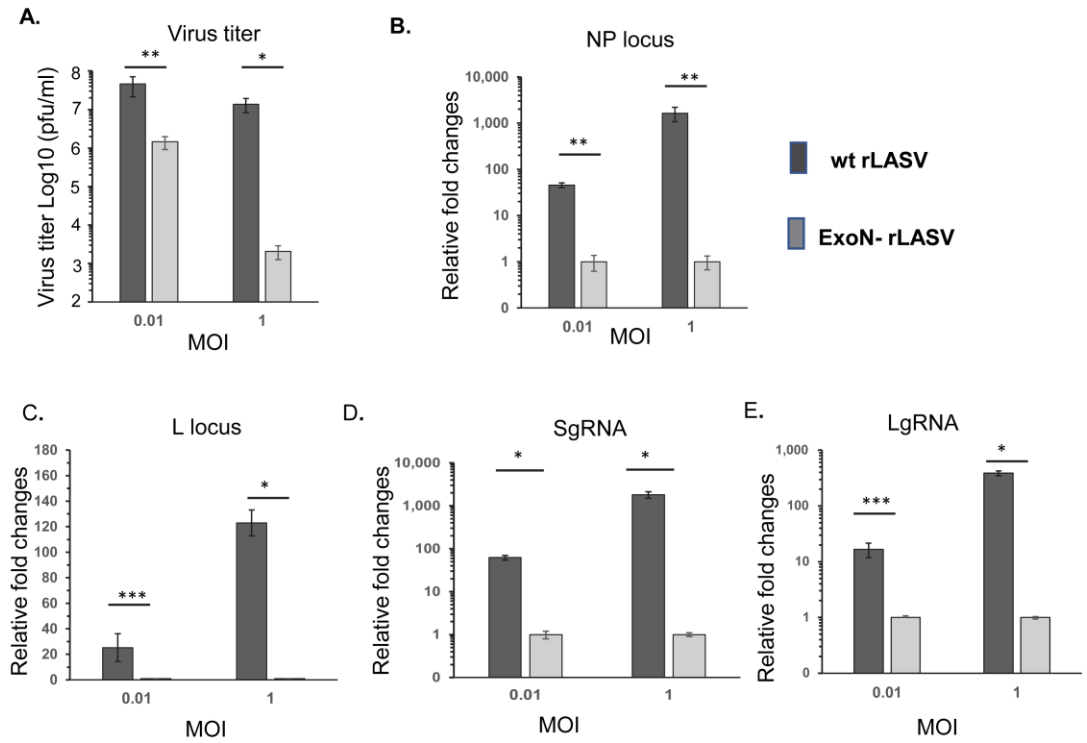
A.
Virus titer
Virus titer Log10 (pfu/ml)
MOI
B.
NP locus
Relative fold changes
MOI
wt rLASV
ExoN- rLASV
C.
L locus
Relative fold changes
MOI
D.
SgRNA
Relative fold changes
MOI
E.
LgRNA
Relative fold changes
MOI

Fig 4

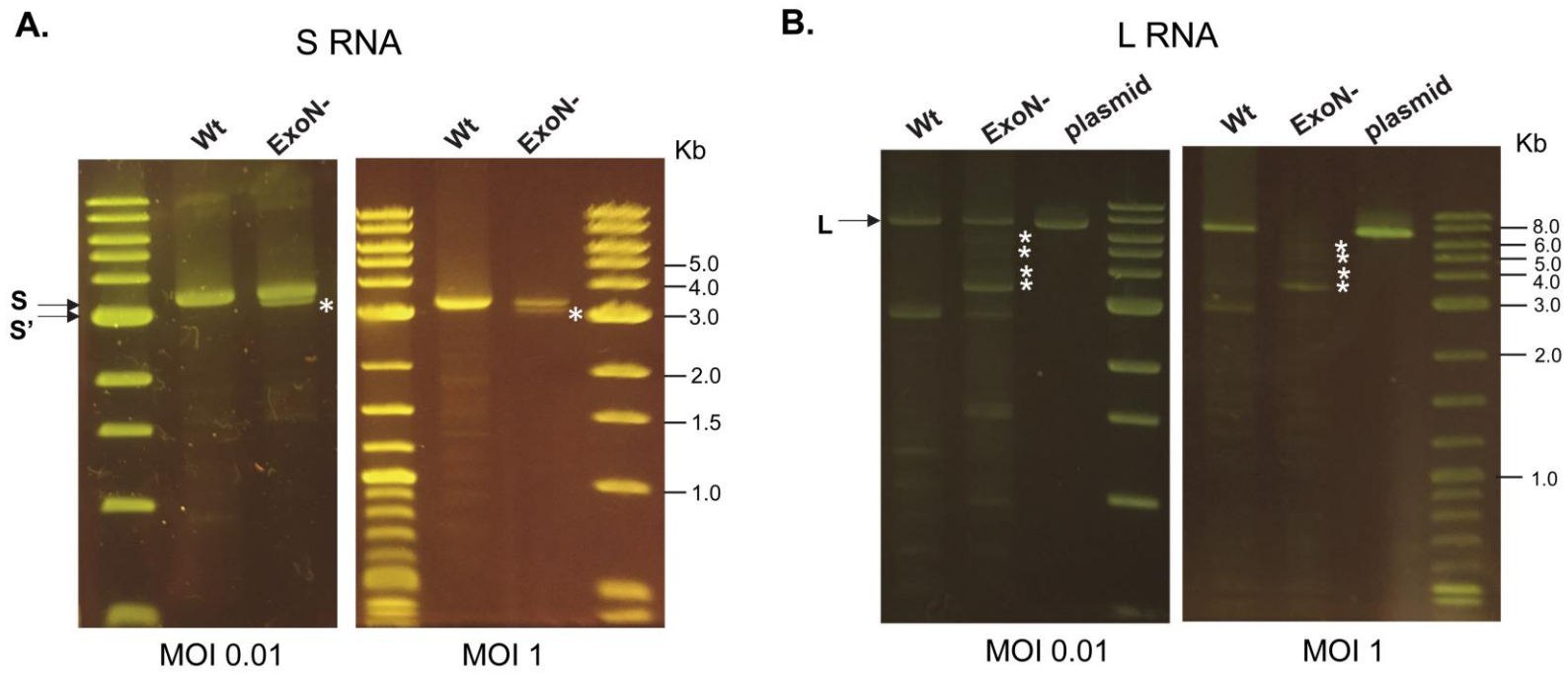
A.
S RNA
Wt
ExoN-
Wt
ExoN-
Kb
S
S'
5.0
4.0
3.0
2.0
1.5
1.0
MOI 0.01
MOI 1
B.
L RNA
Wt
ExoN-
plasmid
Wt
ExoN-
plasmid
Kb
L
8.0
6.0
5.0
4.0
3.0
2.0
1.0
MOI 0.01
MOI 1

Fig 5

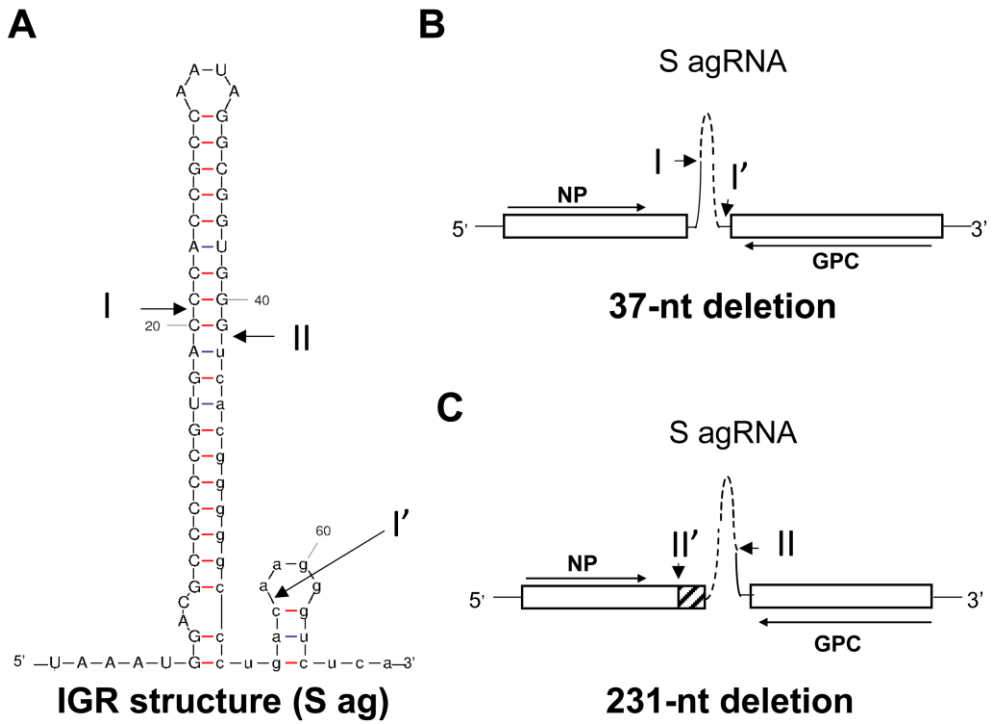
A
I
II
I′
20
40
60
5′ –U–A–A–A–U–G–c–u–g–c–u–c–a–3′
IGR structure (S ag)
B
S agRNA
NP
I
I′
5′
3′
GPC
37-nt deletion
C
S agRNA
NP
II′
II
5′
3′
GPC
231-nt deletion

Fig 6

A.

Sample ID	CCS Reads	Number of CCS Bases	CCS Read Score (mean)	Number of Passes (mean)
Wt rLASV	402,410	933,554,242	0.999	28
ExoN- rLASV	381,134	994,863,239	0.999	26

B.

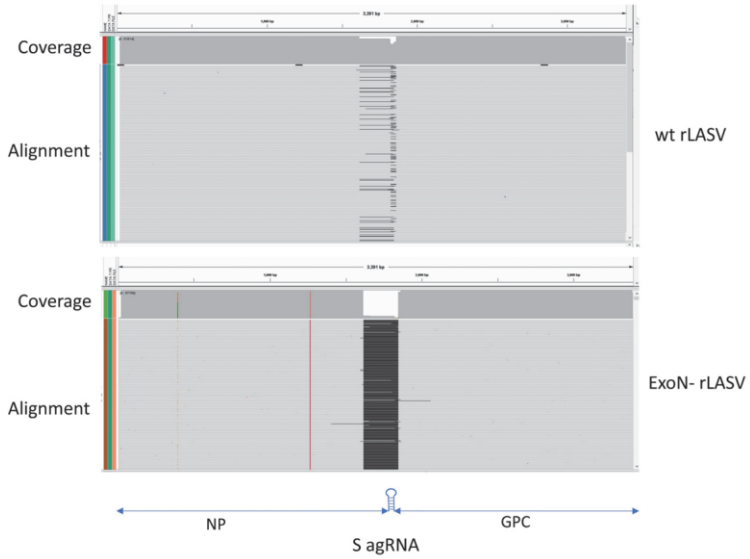

C.

Sample	231-nt del	37-nt del
Wt rLASV	7.1%	18.2%
ExoN- rLASV	88.9%	4.9%

Fig 7

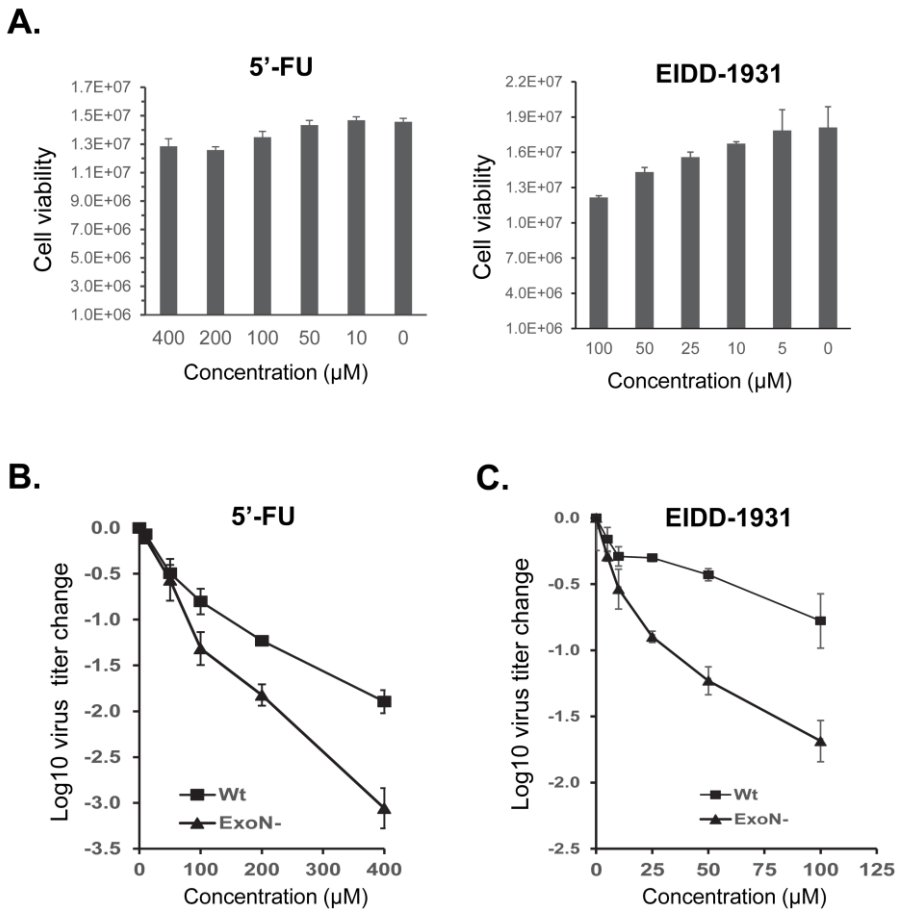
A.
5'-FU
Cell viability
1.7E+07
1.5E+07
1.3E+07
1.1E+07
9.0E+06
7.0E+06
5.0E+06
3.0E+06
1.0E+06
400 200 100 50 10 0
Concentration (μM)
EIDD-1931
Cell viability
2.2E+07
1.9E+07
1.6E+07
1.3E+07
1.0E+07
7.0E+06
4.0E+06
1.0E+06
100 50 25 10 5 0
Concentration (μM)
B.
5'-FU
Log10 virus titer change
0.0
-0.5
-1.0
-1.5
-2.0
-2.5
-3.0
-3.5
0 100 200 300 400
Concentration (μM)
Wt
ExoN-
C.
EIDD-1931
Log10 virus titer change
0.0
-0.5
-1.0
-1.5
-2.0
-2.5
0 25 50 75 100 125
Concentration (μM)
Wt
ExoN-

Fig 8

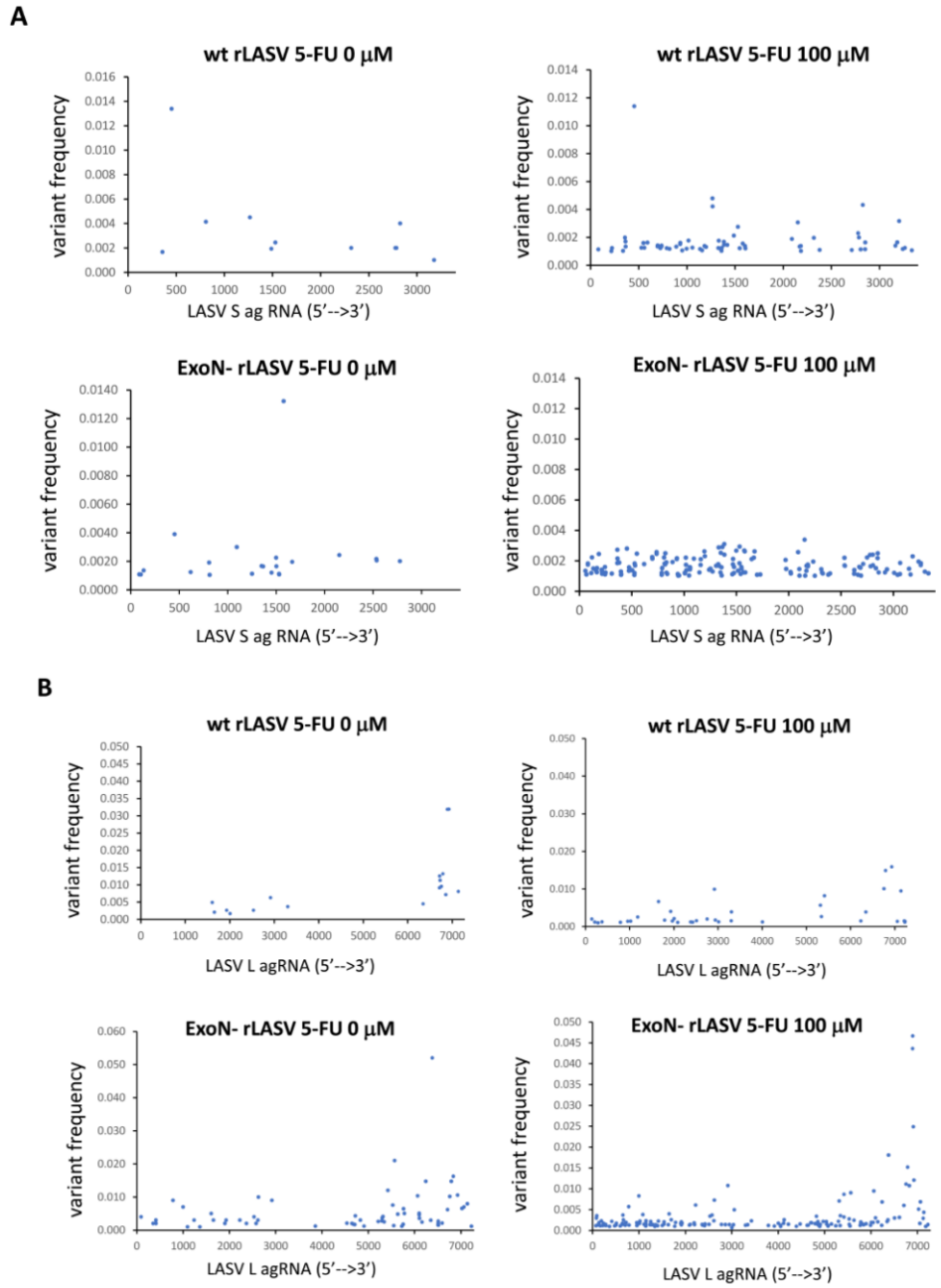
A
wt rLASV 5-FU 0 µM
wt rLASV 5-FU 100 µM
ExoN- rLASV 5-FU 0 µM
ExoN- rLASV 5-FU 100 µM
variant frequency
LASV S ag RNA (5'-->3')
B
wt rLASV 5-FU 0 µM
wt rLASV 5-FU 100 µM
ExoN- rLASV 5-FU 0 µM
ExoN- rLASV 5-FU 100 µM
variant frequency
LASV L agRNA (5'-->3')

Fig 9

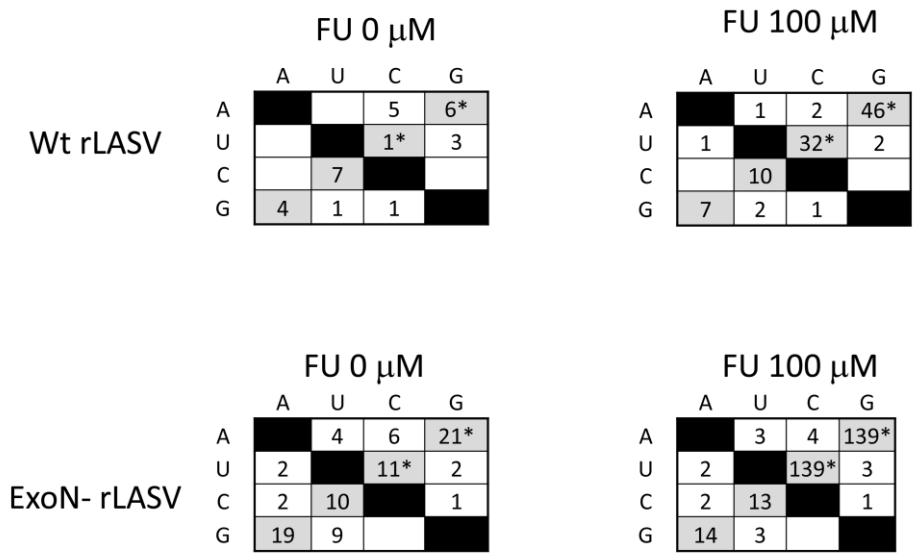
FU 0 μM
FU 100 μM
Wt rLASV
ExoN- rLASV
A U C G
A 5 6*
U 1* 3
C 7
G 4 1 1
A 1 2 46*
U 1 32* 2
C 10
G 7 2 1
A 4 6 21*
U 2 11* 2
C 2 10 1
G 19 9
A 3 4 139*
U 2 139* 3
C 2 13 1
G 14 3

Fig 10

A. The 37-nt deletion in LASV NP ExoN-

(**1**) Mis-incorporation/stop

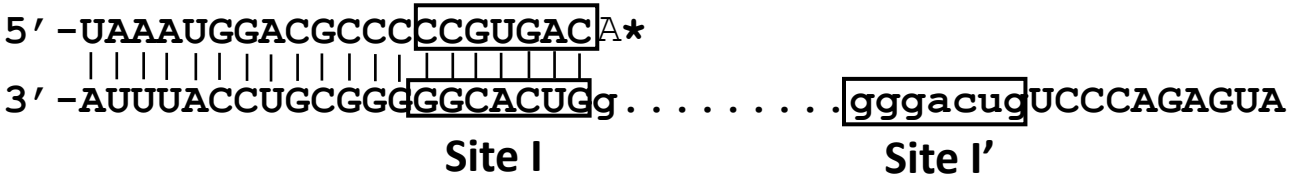

(**2**) Re-align/resume

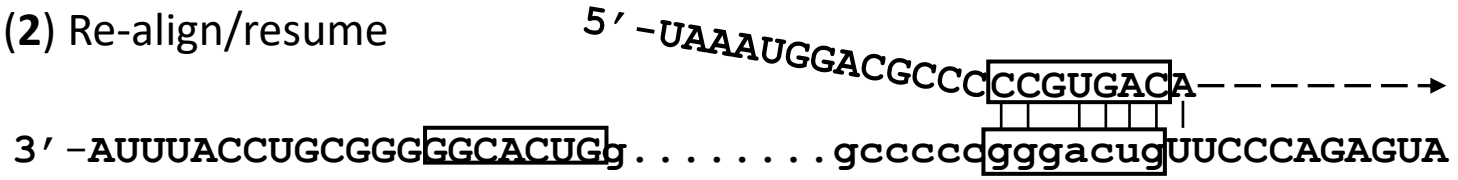

B. The 231-nt deletion in LASV NP ExoN-

(**1**) Mis-incorporation/stop

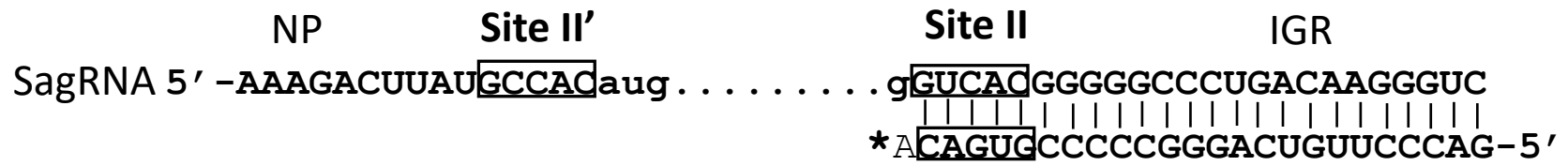

(**2**) Re-align/resume